

# Nanostructured Platinum Electrocatalysts for Fuel Cell Applications: Recent Advances

Gubbala V. Ramesh<sup>1,\*</sup>, T. V. Surendra<sup>1</sup>, N Mahender Reddy<sup>1</sup>, D Saritha<sup>1</sup>, Md. Atif Qaiyum<sup>1</sup>, Megana Boddupally<sup>2</sup>, Indurthi Sriyayathi<sup>2</sup>

<sup>1</sup>Department of Chemistry, Chaitanya Bharathi Institute of Technology, Osman Sagar Rd, Kokapet, Gandipet, Telangana, 500075, India

<sup>2</sup>Department of Chemical Engineering, Chaitanya Bharathi Institute of Technology, Osman Sagar Rd, Kokapet, Gandipet, Telangana, 500075, India.

**Abstract.** The use of Platinum based electro-catalysts is still fundamental in Low Temperature Fuel Cells such as Polymer Electrolyte Membrane (PEM) Fuel Cells due to the exceptional activity and durability of Platinum for Oxygen Reduction Reaction (ORR) in Acidic Conditions. However, the high cost of Platinum, the poor utilization of Platinum, and the significant losses in durability caused by dissolution, aggregation, alloy leach, and corroded supports have been major hindrances to widespread commercialization. This Review Paper will review the advancements in the last decade of Nano Structured Platinum Electro-Catalysts and their Structure Activity Durability (SAD) relationship and compare them to the platinum loadings and mass transport limitations that have been reported historically. In addition, the paper will investigate the effects of particle size, particle shape, dimensionality, alloying, strain engineering, and metal support interaction on the ORR Kinetics and Long-Term Stability of these nano-structures. A particular focus will be placed on one dimensional nano-wire, hollow and open architecture, Pt skin, and core-shell structures, and strong metal-support interactions that inhibit degradation while enhance catalytic activity. The paper will also critique common errors in reporting and benchmarking performance, which include the discrepancy between half-cell level tests and device level tests. Lastly, the paper will discuss design principles and future research direction for the advancement of Platinum Catalysts that are Durable, Scalable and Economically Viable. Ultimately, the purpose of this paper is to provide a platform for the advancement of Platinum Catalysts to Practical Fuel Cell Applications through a combination of mechanistic understanding, realistic testing protocol, and scalable synthesis strategy.

## 1. Introduction

Fuel cells convert the chemical energy of fuel directly into electricity, offering high-efficiency, low-emission power for transportation and stationary applications. Among the

---

\* Corresponding author: [venkataramesh\\_chm@cbit.ac.in](mailto:venkataramesh_chm@cbit.ac.in)

several fuel cell types, polymer-electrolyte-membrane fuel cells (PEMFCs) dominate automotive and portable sectors because of their low operating temperature and high power density. However, the sluggish kinetics of the oxygen-reduction reaction (ORR) at the cathode imposes large overpotentials that degrade efficiency and necessitate large platinum (Pt) loadings [1]. Platinum currently remains the only commercially viable ORR catalyst because of its optimal adsorption energy for ORR intermediates and superior durability, yet Pt accounts for roughly half of the cost of PEMFC stacks [2]. Conventional Pt nanoparticles dispersed on high-surface-area carbon (Pt/C) suffer from low Pt utilization because only the surface atoms are catalytically accessible. More importantly, weak interactions between Pt and carbon supports allow nanoparticles to migrate, dissolve and coalesce during operation, while the carbon support corrodes under start-up/shut-down conditions and high potentials [3]. These degradation processes reduce the electrochemically active surface area (ECSA) and severely limit durability [4].

The central thesis of this review is that electrocatalytic performance and durability of Pt catalysts are governed by nanoscale control of surface atomic structure, electronic states and metal-support interactions rather than Pt loading alone. Recent advances in nanostructured Pt architectures-nanoparticles, shape-controlled nanocrystals, one-dimensional nanowires, two-dimensional ultrathin films, open/hollow frameworks, core-shell and Pt-skin structures-and in alloying, strain engineering and support design have dramatically improved ORR activity and stability. However, these developments also expose trade-offs between activity and durability and highlight challenges in achieving scalable synthesis and realistic performance metrics. This critical review evaluates these advances, emphasising structure-activity-durability relationships, mechanistic insights, design trade-offs and remaining scientific questions. We delineate recent progress in Pt nanostructures, alloying and support effects, discuss degradation mechanisms and benchmarking issues, and propose design principles and research directions toward durable and scalable Pt electrocatalysts.

## **2. Reaction Mechanisms and Structure Sensitivity of Pt Catalysts**

### **2.1 ORR pathways on Pt**

The ORR proceeds either via a four-electron pathway producing  $\text{H}_2\text{O}$  or a two-electron pathway yielding  $\text{H}_2\text{O}_2$ . On Pt surfaces,  $\text{O}_2$  adsorption, electron transfer, O-O bond cleavage and removal of oxygenated intermediates occur sequentially[5]. The four-electron pathway involves dissociative or associative mechanisms depending on whether  $\text{*OOH}$  is formed as an intermediate[6]. In PEMFCs the four-electron route dominates because the proton-rich environment and high overpotential favour complete reduction; nonetheless, partial reduction to  $\text{H}_2\text{O}_2$  occurs under certain conditions and can corrode membranes.

### **2.2 Structure sensitivity and facet dependence**

The intrinsic activity of Pt depends strongly on surface crystallography. Studies using well-defined single crystals reveal that ORR activity increases with step density in the order  $\text{Pt}(100) < \text{Pt}(111) < \text{Pt}(110)$ [7]. Step and kink sites weaken the binding of  $\text{O}^*$  and  $\text{OH}^*$  intermediates, lowering the activation barrier for the rate-determining proton/electron transfer. Caffeine, as a hydrophobic modifier, reduces PtOH formation at both Pt(111) and Pt(110) surfaces through selective adsorption, while increasing ORR performance in comparison to unmodified Pt by up to one order of magnitude.[8]. The effect of alloying Pt

with transition metals also provides a way to further adjust the d-band center; e.g., Pt<sub>3</sub>Ni(111) exhibits a Pt-skin surface with a ~10 times higher intrinsic activity compared to Pt(111) due to the combination of lattice compression and ligand effects which reduce the strength of O\* binding.[1].

Generalised coordination number (GCN) analyses indicate an optimum coordination around 8.3, corresponding to (111) facets with a moderate density of steps[2]. Lower coordination (edges, corners) often increases activity but accelerates dissolution and coalescence, illustrating the activity–stability trade-off. Defect engineering (introducing adatoms, vacancies or step edges via etching or dealloying) can boost intrinsic activity up to 3–4× relative to defect-free Pt(111)[3], but the resulting under-coordinated atoms are prone to dissolution[4].

### 2.3 Intrinsic vs mass activity and the pitfalls of half-cell measurements

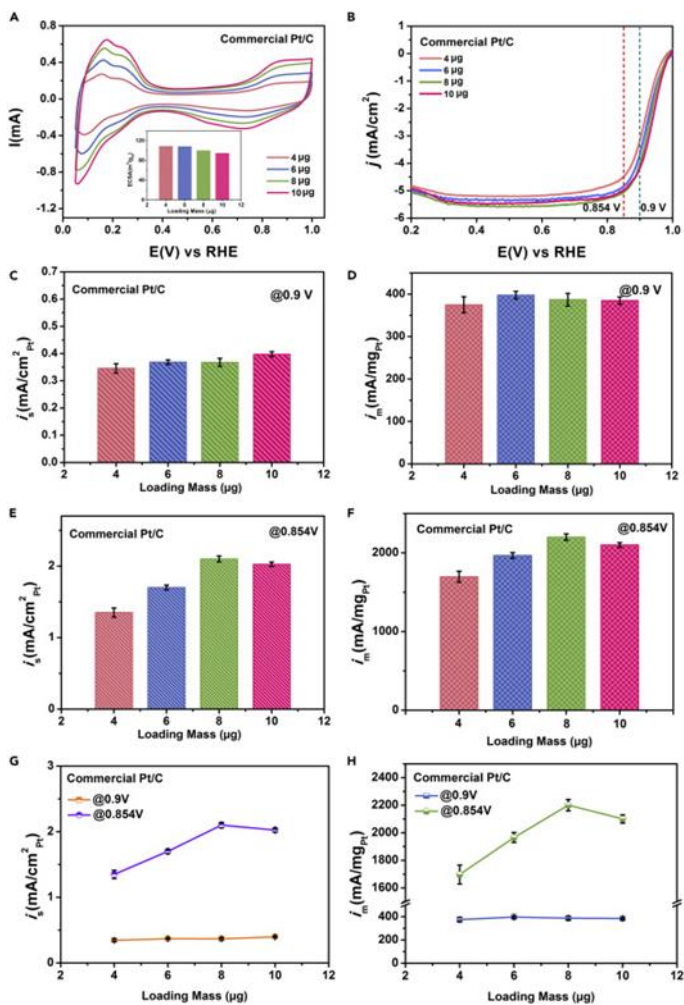


**Fig. 1.** Effect of Pt mass loading on ORR activity of commercial Pt/C measured by RDE. (A) Cyclic voltammograms at different Pt loadings. (B) ORR polarization curves showing kinetic and diffusion-affected regions. (C, D) Specific and mass activities at 0.9 V vs RHE, showing weak dependence on loading. (E, F) Activities at 0.854 V vs RHE, where higher loadings give higher

apparent activity. (G, H) Comparison of loading trends at 0.9 V and 0.854 V, highlighting transport limitations at lower potentials. [9]

RDE measurements are commonly used to screen ORR catalysts. However, the measured activity depends on experimental conditions. Catalyst loading and film thickness strongly affect the current response. As shown in Figure 1, Pt/C displays similar mass activities at 0.9 V vs RHE for Pt loadings between 4 and 10  $\mu\text{g}$ . This potential mainly reflects kinetic control. At 0.854 V vs RHE, the situation changes. Both mass and specific activities increase with loading. This trend indicates increasing diffusion and transport effects. Therefore, activities measured outside the kinetic region may not represent intrinsic catalyst performance. [9] Choosing potentials too close to the diffusion-limiting regime or using thick films leads to overestimation of activity. Tafel analysis indicated that 0.9 V is within the kinetic-control region for typical Pt loadings, whereas 0.854 V is not [6]. Further, a recent perspective highlighted that many studies deviate from Department of Energy (DOE) protocols; inconsistent scan directions, electrolyte purities and film preparation yield irreproducible data [7]. Importantly, RDE measurements are performed under low current and ambient temperature conditions with a liquid electrolyte, whereas membrane-electrode-assembly (MEA) tests involve porous catalyst layers, high gas transport resistance and realistic operating temperatures. Discrepancies between RDE and MEA performance underscore the need for standardised protocols and early MEA validation [8].

### 3. Size, Shape and Dimensionality Effects in Nanostructured Pt

#### 3.1 Pt nanoparticles

Reducing particle size increases the fraction of surface atoms but also alters surface structure. Controlled studies on Pt/C with narrowly distributed particle sizes (1.1–1.8 nm) showed that specific activity remains constant for particles  $>1.8$  nm, increases as size decreases to 1.3 nm and decreases again for particles  $<1.3$  nm [1]. The optimum at  $\sim 1.3$  nm arises from a higher proportion of (110) facets and high-index edges that enhance ORR kinetics. Further reduction leads to dominance of low-coordinated corner atoms which bind oxygen too strongly and reduce activity [2]. Small particles dissolve more readily due to their high surface energy and can migrate and coalesce on carbon supports, leading to Ostwald ripening and loss of ECSA. Therefore, there exists an activity–stability trade-off: decreasing size beyond  $\sim 2$  nm increases activity but accelerates degradation.

#### 3.2 Shape-controlled and facet-engineered Pt

Shape control offers an alternative route to optimize exposed facets without reducing particle size. Cubes exposing (100) facets, octahedra exposing (111) facets and tetrahedra exposing high-index  $\{730\}$  facets have been synthesised using capping agents and seed-mediated growth. A mini-review described that depositing Pt onto Au nanocubes often destroys morphology due to lattice mismatch, but adding trace  $\text{Ag}^+$  ions smooth Pt deposition and yields well-defined Pt@Au cubes; the resulting catalysts exhibited higher ORR onset potentials and improved durability compared with commercial Pt/C [3]. Ultrathin PdPtCu nanorings with high-index facets delivered exceptional ECSA ( $92 \text{ m}^2 \text{ g}^{-1}$ ) and maintained 82 % of their mass activity after 10 000 cycles, outperforming Pt/C [4]. Truncated octahedral Pd@Pt(111) nanoparticles achieved superior mass and specific activities and better stability than tetrahedral or Pt black catalysts [5]. These

examples illustrate that exposing specific facets and constructing core–shell architectures can enhance activity and durability; however, the synthesis often requires delicate control of surfactants and reduction kinetics and may be difficult to scale beyond laboratory conditions[6].

### 3.3 One-dimensional and two-dimensional nanostructures

One-dimensional (1D) Pt nanowires and two-dimensional (2D) ultrathin films reduce grain boundaries and provide continuous pathways for electron transport, improving conductivity and mechanical robustness. Graphene-supported Pt nanowire arrays grown via sulfur-doped graphene templates showed dense coverage of ultrathin (2–5 nm) nanowires and 2–3 times higher ORR and methanol oxidation activities than commercial Pt/C[7]. The doped graphene support provided nucleation sites and high conductivity, enabling uniform nanowire growth and high Pt utilization.

Anisotropic mesoporous Pt@Pt-skin Pt<sub>3</sub>Ni core–shell framework nanowires (CSFWs) combine 1D structures with hollow frameworks. In these catalysts, an atomic-jagged Pt nanowire core is encapsulated by a mesoporous Pt<sub>3</sub>Ni framework with an ultrathin Pt skin. The resulting specific activity at 0.9 V vs RHE reaches 8.42 mA cm<sup>-2</sup>, about 26× higher than commercial Pt/C, and the mass activity of 6.69 A mg<sup>-1</sup> surpasses the 2020 U.S. DOE target by 15×[8]. Remarkably, after 50 000 potential cycles between 0.6 and 1.1 V, the half-wave potential shifted by only 4 mV and the mass activity decreased by 2.8 %, whereas Pt nanowires lost ~32 % of their mass activity after 10 000 cycles and Pt/C suffered ~47 % loss[1]. Transmission electron microscopy showed negligible morphological changes after cycling[2]. The high durability arises from (i) weakened oxygen binding on the Pt-skin surface that suppresses Pt dissolution and carbon corrosion, (ii) multipoint contact between the porous framework and carbon support which inhibits migration and ripening, and (iii) sufficient Pt-skin thickness (≥4 monolayers) that prevents Ni leaching from the inner framework[3]. These results highlight how combining 1D cores, hollow architectures and Pt-skin surfaces can simultaneously achieve ultra-high activity and outstanding durability.

### 3.4 Open and hollow nanostructures

Open structures such as nanoframes, nanocages and hollow nanoparticles maximize Pt utilization by exposing both interior and exterior surfaces while reducing density. Hollow Pt–Ni nanoparticles synthesized via sacrificial SiO<sub>2</sub> templates delivered specific and mass activities of 1.88 mA cm<sup>-2</sup> and 0.49 A mg<sup>-1</sup>, respectively, surpassing commercial Pt/C, and their activity decreased only 35–41 % after accelerated stress tests compared with ~50 % drop for Pt/C[4]. The hollow design eliminates carbon support, thereby avoiding carbon corrosion and mitigating Pt aggregation[5]. Similarly, the use of defective hollow carbon spheres to contain Pt nanoparticles limits their migration and dissolutions; accelerated stress tests demonstrate that Pt dissolution, Ostwald ripening and aggregation increase the size of particles and reduce the ECSA in Pt/C; however, hollow spheres can suppress these effects and therefore, produce a smaller size of the Pt particle and an increased ECSA[6]. However, when completely eliminating carbon from the structure decreases the ability for the structure to be electrically conducting, therefore, using electrically conducting substrates, or integrating electrically conducting oxides into the structure is required. Therefore, the challenge is to balance the structural stability and the scalability of the structure with the electrical conductivity.

## 4. Alloying, Strain and Electronic Structure Engineering

### 4.1 Pt–M alloys and d-band tuning

The incorporation of transition metals into platinum ( $M = \text{Ni, Co, Cu, Fe}$ ) creates changes in Pt's electronic structure through both the ligand effect and the strain effect. Alloy formation reduces the Pt–Pt bond length and d-band center, resulting in weaker adsorption of the reaction intermediates for the oxygen reduction reaction (ORR), thus increasing the catalytic activity. Studies on single crystals demonstrated that the Pt<sub>3</sub>Ni(111) surface with a “Pt-skin” has an intrinsic activity approximately 10 times that of Pt(111) because of compressive lattice strain and the lowering of the d-band center by the Ni[7]. Additionally, Pt<sub>3</sub>Ni octahedral nanoparticles were shown to be highly active; however they suffered from nickel leaching and aggregation upon cycling[8].

DFT simulations of AuxPt<sub>1-x</sub>/Pt(111) surfaces reveal that long-range compressive strain induced by distant Au atoms enhances the activity of Pt sites, whereas adjacent Au atoms generate tensile strain and slightly reduce activity[1]. These findings emphasise that not only composition but atomic arrangement governs ORR activity. Strain can be manipulated via lattice mismatch, core–shell structures or dealloying. Introducing tensile strain often weakens Pt–Pt bonds and destabilises the lattice, leading to poor durability; compressive strain from smaller atoms (Ni, Co) lowers oxygen binding energy to the Sabatier optimum, but dissolution of the less noble metal during operation produces surface reconstruction and performance loss.

### 4.2 Pt-skin and core–shell structures

Dealloying Pt–M alloys often produces a Pt-rich skin over an alloy core. Pt-skin thickness critically determines activity and durability: thin skins (<2 monolayers) expose subsurface alloy atoms that reduce Pt loading but are susceptible to leaching, whereas thick skins ( $\geq 4$  monolayers) preserve alloying effects while protecting the core. In mesoporous Pt@Pt-skin Pt<sub>3</sub>Ni CSFWs, the Pt-skin suppressed Ni leaching and maintained high mass activity after 50 000 cycles[2]. Figure 2 illustrates the formation of Pt-skin core–shell nanowires through controlled dealloying. The structural evolution highlights how a continuous Pt-rich shell can stabilise the alloy framework while retaining high catalytic surface exposure. A different core–shell catalyst prepared by underpotential deposition of Ni and subsequent galvanic replacement to form Pt<sub>3</sub>Ni(Pt-skin) on a Pd core exhibited a Pt specific activity of 16.7 mA cm<sup>-2</sup> and mass activity of 14.2 A mg<sup>-1</sup>-90 and 156 times those of commercial Pt/C-and the Pt<sub>3</sub>Ni(Pt-skin) structure effectively inhibited Ni leaching in accelerated durability tests[3]. Nevertheless, many dealloyed nanoparticles lose activity because of surface restructuring and dissolution of the less noble metal[4], highlighting the need to optimize composition, shell thickness and operating conditions.

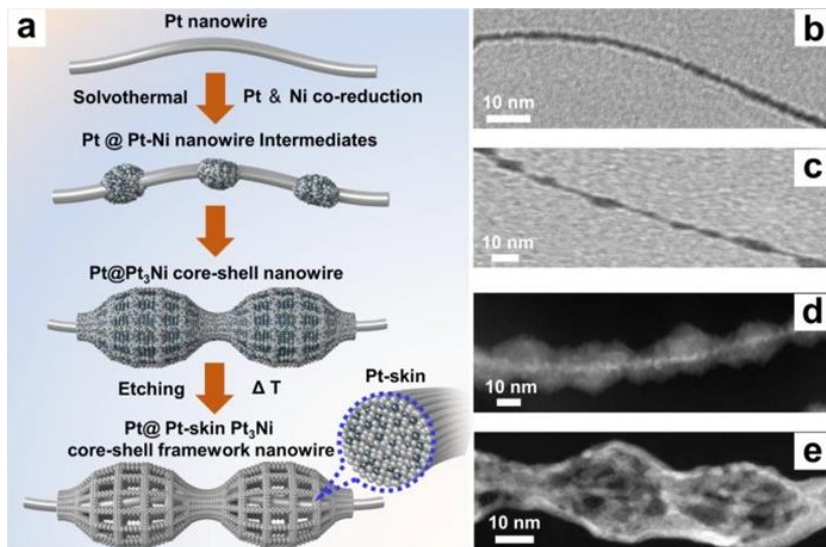


**Fig. 2.** Schematic illustration and electron microscopy images of mesoporous Pt@Pt-skin Pt<sub>3</sub>Ni core-shell framework nanowires. (a) Proposed synthesis pathway involving Pt–Ni co-reduction, core–shell formation, and dealloying to generate a Pt-rich skin. (b–e) TEM and STEM images showing nanowire morphology, porosity development, and formation of a continuous Pt-skin layer after etching and thermal treatment. [2]

### 4.3 Strain and defect engineering trade-offs

Defect engineering-creating vacancies, adatoms or steps via etching, dealloying or thermal treatment-can increase the coordination environment and strain state of Pt atoms. Defective surfaces with generalised coordination numbers around 8.3 show up to 3.5× higher activity but suffer reduced stability due to increased dissolution [5]. High-index facets such as {210} or {730} offer abundant step sites but are difficult to synthesize reproducibly and degrade under potential cycling. Careful tuning of defect density and strain is needed to approach the volcano optimum without compromising durability.

## 5. Support Effects and Metal–Support Interactions

### 5.1 Limitations of carbon supports

High-surface-area carbon black provides excellent conductivity and allows dispersion of Pt nanoparticles; however, its weak interaction with Pt leads to nanoparticle migration, dissolution and Ostwald ripening, while carbon corrosion under high potentials and acidic conditions causes support collapse [6]. Carbon corrosion generates quinone/hydroquinone redox couples and accelerates Pt detachment and agglomeration [7]. These failure modes necessitate alternative supports or stronger interactions.

### 5.2 Alternative supports and strong metal–support interaction (SMSI)

Graphitic carbon nitride (g-C<sub>3</sub>N<sub>4</sub>), transition metal oxides (TMOs), carbides (TMCs), nitrides (TMNs), 2D metal–organic frameworks (MOFs) and covalent organic frameworks (COFs) have been explored as corrosion-resistant supports [8]. The strong metal–support

interaction (SMSI) arises when reducible oxides partially cover Pt nanoparticles, minimising surface energy and inducing interfacial electron transfer and structural reconstruction [1]. SMSI can modulate adsorption energies and encapsulate nanoparticles, improving activity and stability [2]. For example, TiO<sub>2</sub>, WO<sub>3</sub> or NbO<sub>x</sub> supports generate electron-rich Pt that weakens O\* adsorption and inhibits dissolution. However, SMSI often requires high-temperature reduction to activate the oxide, which can cause sintering and reduce surface area, and metal oxides generally have lower conductivity than carbon. Hybrid supports combining N-doped carbon with metal oxides seek to balance conductivity and stability.

### 5.3 Carbon corrosion and hollow supports

Defective hollow carbon spheres confine Pt nanoparticles within robust shells. Accelerated stress tests show that Pt dissolution, Ostwald ripening and particle detachment enlarge Pt/C particle sizes and reduce ECSA, whereas hollow spheres maintain smaller particle sizes and higher ECSA[3]. The confinement effect and low oxygen functionalisation reduce Pt dissolution but cannot prevent carbon corrosion entirely. Carbon corrosion produces redox couples that degrade performance and is exacerbated by high potentials and load cycling[4]. Moving towards carbon-free supports, such as hollow Pt-Ni nanoparticles or Pt on titanium oxides, eliminates carbon corrosion and simplifies water management but requires conductive networks to compensate for the loss of carbon conductivity [5].

## 6. Durability, Degradation Mechanisms and Operando Insights

Nanoparticles undergo several degradation mechanisms during start-up/shut-down, potential cycling and long-term operation. High potentials oxidize Pt to Pt<sup>2+</sup>, which dissolves into the electrolyte and may redeposit elsewhere, causing particle growth and ECSA loss. Dissolution increases with under-coordinated atoms and acidic conditions [6]. Small particles dissolve and redeposit onto larger ones; migration along the carbon surface leads to coalescence. Hollow carbon supports restrict migration and maintain smaller particle sizes [7]. Under start-up/shut-down and load cycling, carbon oxidizes to CO<sub>2</sub>, collapsing the catalyst layer and detaching Pt nanoparticles [8]. These degradation pathways are reflected in accelerated durability tests. As shown in Figure. 3, structural design strongly influences activity retention during potential cycling. Carbon-free hollow or oxide supports mitigate this but may reduce conductivity. Less noble metals (Ni, Co) dissolve, leading to structural reconstruction and loss of strain and ligand effects. Pt<sub>3</sub>Ni octahedra exhibit high activity but lose Ni and ECSA during cycling [1]. Pt-skin structures with sufficient thickness inhibit Ni leaching [2]. Accelerated stress tests (ASTs) using RDE provide useful comparisons but do not fully replicate the transient potentials, humidity, and reactant gradients in MEAs. Operando techniques such as X-ray absorption spectroscopy, scanning transmission electron microscopy and ambient-pressure X-ray photoelectron spectroscopy reveal real-time changes in oxidation state, coordination environment, and nanoparticle morphology. For example, in situ microscopy shows that Pt nanoparticles in hollow carbon spheres remain confined after cycling [3], while Pt/C shows significant growth. Combining operando insights with advanced modelling will guide rational design of robust catalysts.

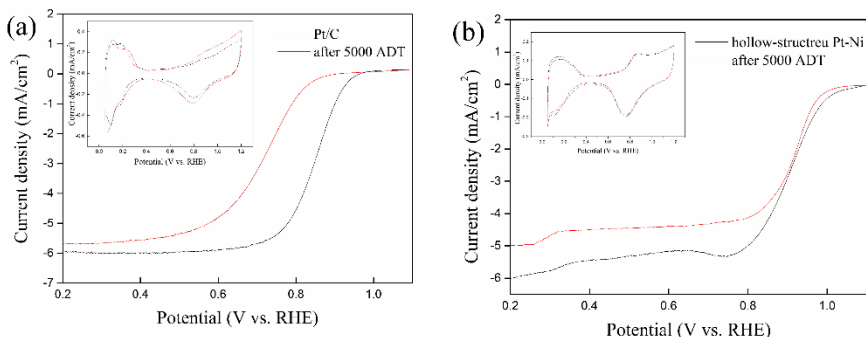


**Fig. 3.** Electrochemical stability comparison before and after accelerated durability testing (ADT). (a) CV and ORR polarization curves of commercial 20 wt% Pt/C recorded initially and after 5000 potential cycles. (b) Corresponding CV and polarization curves for a hollow-structured Pt–Ni catalyst, showing improved retention after cycling. [8]

## 7. Conclusions

Recent advances in nanostructured Pt electrocatalysts have delivered remarkable improvements in ORR activity and durability. Size-controlled nanoparticles, shape-engineered nanocrystals, 1D nanowires, hollow frameworks, and Pt-skin core–shell alloys exploit facets, strain and defect engineering to optimise adsorption energetics. Alloying Pt with transition metals and constructing Pt-skin or core–shell architectures modulate the d-band and lattice strain, while strong metal–support interactions and carbon-free supports mitigate dissolution and corrosion. Mesoporous Pt@Pt-skin Pt<sub>3</sub>Ni core–shell nanowires exemplify the synergy of structural design, achieving mass activities >6 A mg<sup>-1</sup> and retaining performance after 50000 cycles. However, many high-activity catalysts falter under realistic conditions owing to metal leaching, support degradation or fabrication complexity.

The next steps toward large-scale production will require scientists to make commercially viable catalysts durable and easily made in large quantities. The development of standardized methods for testing catalyst performance, validating the results obtained from microelectrode arrays (MEAs), and evaluating long-term stability of catalysts is essential to identifying which catalysts are most promising. To advance catalyst development, future research should focus on developing scalable methods for synthesizing catalysts with controlled structures; rationally designing alloys and supports; integrating characterizations that allow the study of catalysts in operation; and using data-driven approaches to understand the relationship between catalyst structure, activity, and durability. Although platinum is scarce, by carefully structuring nanoparticles and supporting them well, it is possible to maximize their use and minimize their loadings, making it easier to deploy fuel cells more broadly.

## References

1. V. R. Stamenkovic, B. Fowler, B. S. Mun, G. Wang, P. N. Ross, C. A. Lucas and N. M. Markovic, Improved oxygen reduction activity on Pt<sub>3</sub>Ni(111) via increased surface site availability, *Science*, 2007, 315, 493–497. <https://doi.org/10.1126/science.1135941>

2. H. Jin, Z. Xu, Z.-Y. Hu, Z. Yin, Z. Wang, Z. Deng, P. Wei, S. Feng, S. Dong, J. Liu, S. Luo, Z. Qiu, L. Zhou, L. Mai, B.-L. Su, D. Zhao and Y. Liu, Mesoporous Pt@Pt-skin Pt<sub>3</sub>Ni core-shell framework nanowire electrocatalyst for efficient oxygen reduction, *Nature Communications*, 2023, 14, 1518. <https://doi.org/10.1038/s41467-023-37268-4>
3. M. Chen, Strong metal-support interaction of Pt-based electrocatalysts with transition metal oxides/nitrides/carbides for oxygen reduction reaction, *Microstructures*, DOI:10.20517/microstructures.2023.12. <https://doi.org/10.20517/microstructures.2023.12>
4. S. S. Kocha, K. Shinozaki, J. W. Zack, D. J. Myers, N. N. Kariuki, T. Nowicki, V. Stamenkovic, Y. Kang, D. Li and D. Papageorgopoulos, Best practices and testing protocols for benchmarking ORR activities of fuel cell electrocatalysts using rotating disk electrode, *Electrocatalysis*, 2017, 8, 366–374. <https://doi.org/10.1007/s12678-017-0378-6>
5. H. Yano and K. Iwasaki, Size-Dependence of the electrochemical activity of platinum particles in the 1 to 2 nanometer range, *Surfaces*, 2024, 7, 472–481. <https://doi.org/10.3390/surfaces7030030>
6. N. Hoshi, M. Nakamura, R. Kubo and R. Suzuki, Enhanced oxygen reduction reaction on caffeine-modified platinum single-crystal electrodes, *Communications Chemistry*, 2024, 7, 23. <https://doi.org/10.1038/s42004-024-01113-6>
7. H. Yu, M. J. Zachman, K. S. Reeves, J. H. Park, N. N. Kariuki, L. Hu, R. Mukundan, K. C. Neyerlin, D. J. Myers and D. A. Cullen, Tracking Nanoparticle Degradation across Fuel Cell Electrodes by Automated Analytical Electron Microscopy, *ACS Nano*, 2022, 16, 12083–12094. <https://doi.org/10.1021/acsnano.2c02307>
8. Q. Wang, B. Mi, J. Zhou, Z. Qin, Z. Chen and H. Wang, Hollow-Structure Pt-Ni Nanoparticle electrocatalysts for oxygen reduction reaction, *Molecules*, 2022, 27, 2524. <https://doi.org/10.3390/molecules27082524>
9. W. Chen, Q. Xiang, T. Peng, C. Song, W. Shang, T. Deng and J. Wu, Reconsidering the benchmarking evaluation of catalytic activity in oxygen reduction reaction, *iScience*, 2020, 23, 101532. <https://doi.org/10.1016/j.isci.2020.101532>